



Article

# Estimation on Fixed-Bed Column Parameters of Breakthrough Behaviors for Gold Recovery by Adsorption onto Modified/Functionalized Amberlite XAD7

Adina Negrea <sup>1</sup>, Maria Mihailescu <sup>1,2</sup>, Giannin Mosoarca <sup>1,\*</sup>, Mihaela Ciopec <sup>1,\*</sup>,  
Narcis Duteanu <sup>1</sup>, Petru Negrea <sup>1</sup> and Vasile Minzatu <sup>2</sup>

<sup>1</sup> Faculty of Industrial Chemistry and Environmental Engineering, Politehnica University Timisoara, Bd. V. Parvan No. 6, 300223 Timisoara, Romania; adina.negrea@upt.ro (A.N.); mihailescumia@gmail.com (M.M.); narcis.duteanu@upt.ro (N.D.); petru.negrea@upt.ro (P.N.)

<sup>2</sup> Research Institute for Renewable Energy of the Politehnica University Timisoara, 138 Musicescu Street, 300774 Timisoara, Romania; vasile.minzatu@student.upt.ro

\* Correspondence: giannin.mosoarca@upt.ro (G.M.); mihaela.ciopec@upt.ro (M.C.);  
Tel.: +40-25-640-4185 (G.M.); +40-25-640-4192 (M.C.)

Received: 17 August 2020; Accepted: 18 September 2020; Published: 20 September 2020



**Abstract:** The objective of this paper was to evaluate the potential of a new adsorbent material to recover Au (III) from real wastewater, in a column with a fixed bed in a dynamic regime. The material was obtained through functionalization, by impregnation of the commercial resin, Amberlite XAD 7 type, with L-glutamic acid, which has active groups  $-NH_2$  and  $-COOH$ . The goal of the experiments was to follow the correlation of fixed-bed column specific adsorption parameters (the effluent volume, the amounts of adsorbent, heights of the adsorbent layer in column) with the time necessary to cross the column. The experimental data obtained were modeled, using the Bohart–Adams, Yoon–Nelson Thomas and Clark models, to establish the mechanism of the Au (III) recovery process, in a dynamic regime. Also, we established the number of cycles for adsorption–desorption for which the new material can be used. We used 5%  $HNO_3$  (5%) as desorption agent in five adsorption–desorption cycles, until the process was no longer efficient. The degree of desorption varied between 84% and 34% from cycle 1 to cycle 5.

**Keywords:** gold recovery; acid L-glutamic; fixed-bed column; adsorption; breakthrough curves modelling

## 1. Introduction

Adsorption is defined as a process determined by increasing a specific compound concentration at the interface of two phases [1]. In a first stage, the compounds from the solution are transported from one phase to another and, subsequently, they adhere to the surface. The process is complex and depends on the chemistry of the surface or the sorbent and sorbate nature, as well as the nature of the solid–liquid system. Thus, adsorption of metal ions from wastewater is a cheap, efficient, non-toxic and environmentally friendly process [2,3].

There are two types of adsorption processes with good efficiency: adsorption in batch system and column adsorption. In the batch system, adsorption takes place between the two liquid–solid phases, where the solid phase moves continuously along with the liquid phase. The main advantages of this process are: (i) the adsorbent and the adsorbate are constantly mixed and the volume of the solution is constant; (ii) is an easy and economical method, being used in many studies. The disadvantage of

this technique is that, in industry, it is not recommended to work with small amounts of adsorbent material. This makes it difficult to remove and/or recover a small amount of metal ions.

Among the adsorption processes in the column, the adsorption in a fixed bed presents some important advantages: (i) the process is continuous because the adsorbent is continuously in contact with the adsorbent; (ii) it is simple and has low costs; (iii) it can be used on an industrial scale. The disadvantages of the fixed-bed column process are: during the adsorption process, preferential routes can be formed, the adsorption being non-uniform; and the concentration profiles vary in space and time, which makes it very difficult to optimize and design the technique without a quantitative approach [4,5].

Gold is a precious, anticorrosive, ductile, highly malleable metal, with unique physical and chemical properties used in the electrical and electronic industry as well as in the manufacture of jewelry and coins [6–8].

Besides the adsorption process, there are a variety of Au (III) recovery methods, including: mechanical separation, hydrometallurgy, biohydrometallurgy [9–12], cementation, coagulation, solvent extraction, ion exchange, gravitational separation, flotation [8]. These methods have a number of disadvantages: (i) large amounts of sludge are generated; (ii) strongly acidic or basic solutions are used; (iii) if algae, bacteria and fungi (which have the ability to accumulate gold) are used, their multiplication must be controlled; (iv) the gold obtained has impurities requiring its purification; (v) a high cost of the operation [13–17].

Given the increasing number of environmental accidents due to the application of these gold-recovery technologies, scientists are looking for environmentally friendly technologies, such as adsorption [18]. The recovery process only makes sense if the cost of recovery is much lower than the value of the recovered gold. In addition, the restrictions imposed by waste management and strict environmental regulations require that the technological options chosen for gold recovery be economically viable and environmentally friendly. The advantage of adsorption is that gold can be recovered in small quantities from either primary or secondary solutions. Adsorption is easy to apply and if the adsorbent material is well chosen, it can have efficiencies that should not be neglected [19–24].

Regarding the recovery of Au (III), the adsorption process is the most suitable, the adsorbing properties of the material used being very important. The active groups from the adsorbent structure play an important role because they have the ability to bind by complexation, ionic bonds, hydrogen bond or electrostatic attraction.

This paper aims to recover Au (III) from solutions generated by the galvanic coating stage within the process of obtaining printed circuit boards (PCBs) used in electronic circuits. The recovery of Au (III) in this case is achieved by adsorption in dynamic regime, in the column with a fixed bed. Thus, the aim is to establish the Au (III) recovery mechanism by adsorption in a dynamic regime, in fixed-bed column, using a newly obtained material by functionalization by the solvent impregnated resin—SIR method [25] of a cheap, commercial resin, Amberlite XAD7 with L-glutamic acid, whose pending groups are  $-\text{NH}_2$  and  $-\text{COOH}$ . The material is selective, relatively inexpensive, environmentally friendly, adsorbent, and was used with good results for recovering gold from dilute solutions in a batch system [26]. At the same time, the number of adsorption–desorption cycles at which the new material can be used was established.

## 2. Materials and Methods

The surface morphology of the material obtained according to the information presented in the specialized literature [26] was studied using a scanning electron microscope Quanta FEG 250 at 500× magnification. Adsorption experiments were realized in a dynamic regime, in a fixed-bed column. The initial concentration of Au (III) on the wastewater was 60 ( $\text{mg L}^{-1}$ ), being obtained by the dilution of a residual solution from cyanide baths, with an Au (III) concentration of approximately 2000 ( $\text{mg L}^{-1}$ ). Dilution was necessary to avoid rapid depletion of the adsorbent material, but also to highlight the fact that even in smaller quantities, Au (III) can be recovered with good efficiency. For the

dynamic adsorption of Au (III) a column with a diameter of 2 cm and a length of 30 cm was used. The wastewater was pumped at the top of the column using a peristaltic pump (Heidolph SP quick) with a flow rate of 10 (mL min<sup>-1</sup>) and crossed in a downstream direction through the material obtained from the commercial resin of the Amberlite XAD7 type functionalized by impregnation with L-glutamic acid (XAD7-AcG). The column was loaded, sequentially, with layers of different material heights (10, 5 and 3 cm) equivalent to different masses of material (10, 5 and 3 g). Figure 1 shows the scheme of experimental installation used for Au (III) removal in the fixed-bed adsorption column. The flow in the column is kept constant and the discharge flow rate is adjusted so that its adsorption takes place as a stationary dynamic process and the adsorbent material in the column remains continuously covered with solution.

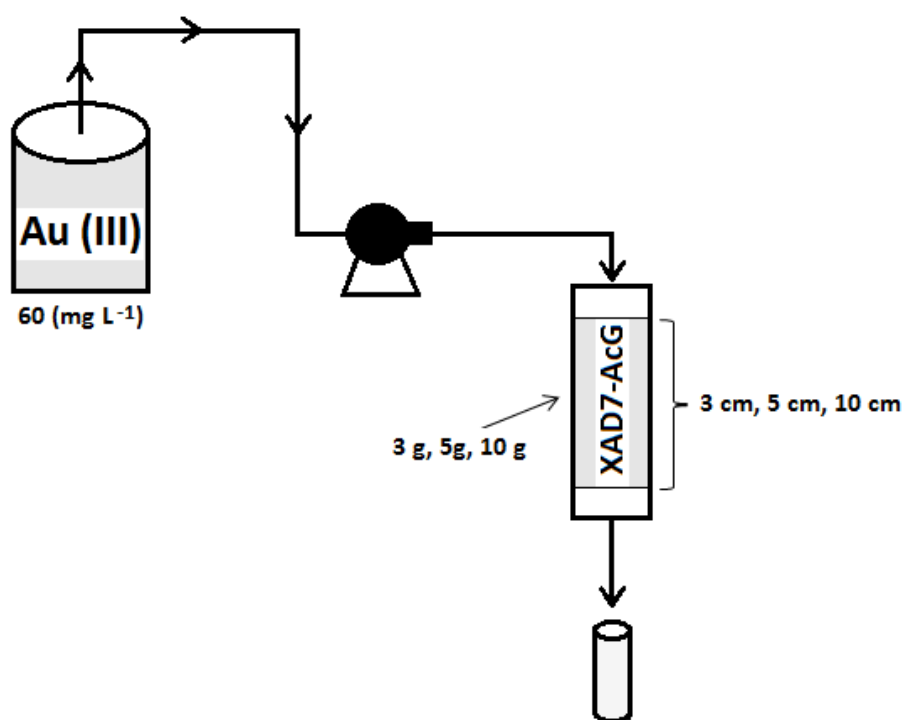


**Figure 1.** The scheme of experimental installation used for Au (III) removal in a fixed-bed adsorption column.

Samples of 25 mL were taken from the effluent at certain intervals. The residual concentration of Au (III) was determined by atomic absorption spectrophotometry, using a Varian SpectrAA 110 atomic absorption spectrophotometer.

In order to determine the number of adsorption–desorption cycles at which the new adsorbent material can be used, after each adsorption cycle (for sample with amount of adsorbent 10 g and the Au (III) initial concentration of solution 60 mg g<sup>-1</sup>), the desorption was performed by introducing into the column as eluent HNO<sub>3</sub> 5%, with a flow rate of 8 (mL min<sup>-1</sup>).

### 3. Results and Discussion

#### 3.1. XAD7-AcG Material Characterization

Figure 2 illustrate the surface morphology of the XAD7-AcG material before and after impregnation with L-glutamic acid. After impregnation, morphological changes specific to the presence of L-glutamic acid appear on the surface of Amberlite XAD7 particles.

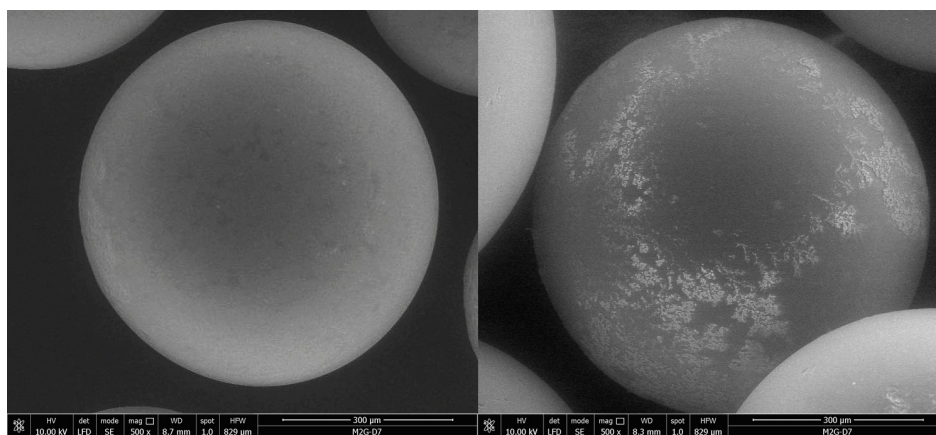


**Figure 2.** Scanning electron microscopy (SEM) for XAD 7-AcG material: (a) before impregnation; (b) after impregnation.

Resin surface functionalization has also been demonstrated by other physico-chemical methods such as Fourier-transform infrared spectroscopy (FTIR) and energy-dispersive X-ray spectroscopy (EDX) in another previous study [26]. EDX reveals the presence of a small amount of nitrogen (5.83%), specific for the  $\text{NH}_2$  group and the FT-IR spectrum highlighted the presence of powerful vibrations specific to the Amberlite XAD7 support and L-glutamic acid respectively.

### 3.2. Fixed-Bed Column Adsorption Studies

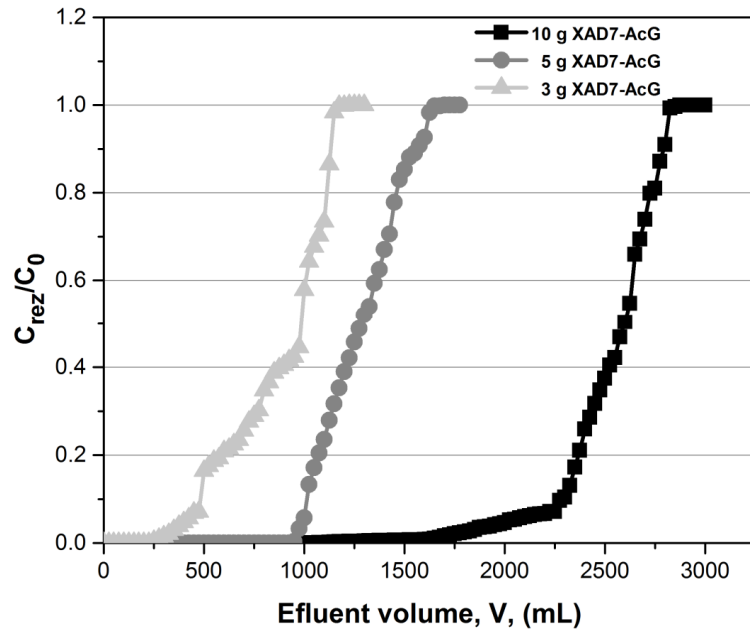
#### 3.2.1. Mass Transfer Zone

During the adsorption process, a large number of metal ions are concentrated on the surface of the adsorbent material, respectively at the interface between the two phases, with an accumulation process taking place. The adsorption of the metal ions on the adsorbent is realized with maximum efficiency if: (i) the transport of the metal ions to the surface of the immobile layer is adequate, transport that can be realized by diffusion or dispersion; (ii) the metal ion transfer occurs at the level of the adsorbent interface; (iii) intraparticle diffusion takes place by moving the solution ions into the adsorbent pores [27].

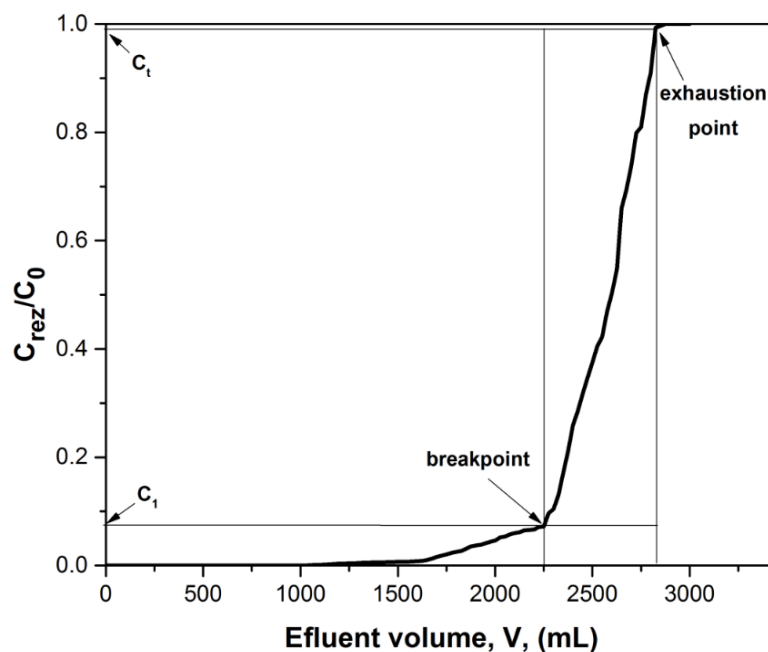
The performances of the adsorption process in the fixed-bed column are highlighted by the study of the breakthrough curves [28,29], which means following the evolution of the ratio between the residual concentration of Au (III) and its initial concentration ( $C_{\text{rez}}/C_0$ ) according to the volume of effluent passed through the column, for three distinct quantities of material, respectively 3, 5 and 10 g (Figure 3).

Figure 4 shows the case of the column in which 3000 mL of wastewater, with an Au (III) concentration of  $60 \text{ mg L}^{-1}$ , were passed over 10 g of XAD7-AcG material. The mass transfer zone (MTZ) is the active surface of the XAD7-AcG material where the Au (III) adsorption takes place. The waste solution Au (III) passes over a new and unused material. At the top of the column, XAD7-AcG material adsorbs Au (III) ions as soon as they come into contact; the area is called the primary sorption zone (PSZ) being delimited between the residual concentration of Au (III) at time 1 (one),  $C_1$ , and the residual concentration of Au (III) at time  $t$ ,  $C_t$ . Thus, the first part of the liquid that is collected is without Au (III) ions, which means in this area the residual concentration of Au (III) tends towards zero. As the volume of Au (III) solution passing through the column increases, an adsorption zone begins to be defined in which mass transfer (MTZ) occurs. In this area, the adsorption process is complete, the concentration of Au (III) ions varies from the initial concentration ( $60 \text{ mg L}^{-1}$ ) to zero, the saturation of the adsorbent material being total. This adsorption area extends over the entire height of the column depending on the contact time. The residual concentration at a given time,  $C_{\text{rez}}$ , is zero and therefore the ratio  $C_{\text{rez}}/C_0$  is zero. When the residual solution passes through the whole

layer of the adsorbent material, reaching its lower part, the Au (III) ions can no longer be completely adsorbed due to the saturation of the material. This moment is called the breakpoint moment and the surface obtained corresponds to the breakpoint curve. After a while, the column is completely saturated or exhausted and the adsorption of Au (III) is no longer performed. In this case the  $C_{rez}/C_0$  ratio is 1 (one) [30–32].



**Figure 3.** Breakthrough curves on Au (III) removal in the fixed-bed column, at various amounts of adsorbent material.



**Figure 4.** A representation of the breakthrough curve with mass transfer zone (MTZ) at an amount of 10g adsorbent material inserted in the column.

### 3.2.2. Adsorption Models for Column Study

The important parameters for evaluating the efficiency of an adsorbent material used in a dynamic regime are: the flow of the effluent in the column, the height of the fixed layer, and the contact time [1,33].

In the adsorption column, phenomena of axial dispersion, external resistance of the film and resistance to intraparticle diffusion can appear. Thus, the mathematical correlation of axial dispersion, mass transfer and intraparticle diffusion is rendered by mathematical models. In order to determine the adsorption mechanism of Au (III) and to design the adsorption process in a dynamic regime it is necessary to know the evolution of the residual concentration of the effluent in time. In this case, four models can be used, namely the Adams–Bohart, Yoon–Nelson, Thomas and Clark models to analyze the breakthrough curves and for the prediction of dynamic nature of the column [34].

The Bohart–Adams Model [35] is used to describe the first part of the column breakpoint curve. The Bohart–Adams equation is linearly expressed as:

$$\ln\left(\frac{C_t}{C_0}\right) = k_{BA}C_0t - k_{BA}N_0\frac{Z}{F}$$

where:  $C_0$ —is the influent concentration, ( $\text{mg L}^{-1}$ );  $C_t$ —is the effluent concentration, ( $\text{mg L}^{-1}$ );  $t$ —is time, (min);  $k_{BA}$ —is the kinetic constant of the Bohart-Adam model, ( $\text{L mg}^{-1} \text{min}^{-1}$ );  $F$ —is the linear velocity calculated by dividing the flow rate by the column section area, ( $\text{cm min}^{-1}$ );  $Z$ —is the bed height of column, (cm);  $N_0$ —is the saturation concentration, ( $\text{mg L}^{-1}$ ).

In Figure 5, the dependence  $\ln(C_t/C_0) = f(\text{time})$  was plotted. The results show that with the increase of the material layer height, respectively with the increase of the amount of material, there is a decrease of the  $N_0$  value, but also an increase of the  $k_{BA}$  value. The obtained regression coefficients  $R^2$  show that the model is not the most suitable to describe the mechanism of the dynamic adsorption process of Au (III) on the XAD7-AcG material [36].

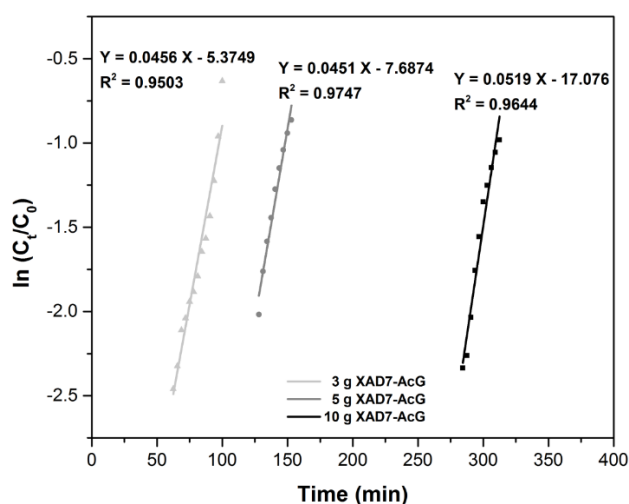


**Figure 5.** Bohart–Adams plots for the adsorption of Au (III) in the fixed-bed column, at various amounts of adsorbent material.

The Yoon–Nelson Model [37] is generally adopted to describe the breakpoint curve. It is a model used especially for the single component system and does not require information about the adsorbent, such as type, physical properties or other characteristics.

The Yoon–Nelson equation is linearly expressed as:

$$\ln\left(\frac{C_t}{C_0 - C_t}\right) = k_{YN}t - \tau k_{YN}$$

where:  $C_t$ —is the solution concentration at time  $t$ , ( $\text{mg L}^{-1}$ );  $C_0$ —is initial solution concentration, ( $\text{mg L}^{-1}$ );  $k_{YN}$ —is the rate constant, ( $\text{min}^{-1}$ );  $\tau$ —is the time required for 50% adsorbate breakthrough, ( $\text{min}$ ).

The parameters  $\tau$  and  $k_{YN}$  can be obtained from the plot of the function  $\ln [C_t/(C_0 - C_t)] = f(\text{time})$ , (Figure 6). It is observed that with the increase of the height of adsorbent layer the time required to breakthrough increases, but not in direct proportion with the adsorbent layer height. The experimental data show that the most efficient layer is the one in which 5 g of adsorbent material is used, because when the adsorbent mass doubles,  $\tau$  does not become double. This fact may be due to the higher probability of preferential drainage channels occurring with the increasing amount of adsorbent material. The regression coefficient  $R^2$  is closer to 1, but we cannot say that the adsorption process mechanism is described in the best way by this model [34].

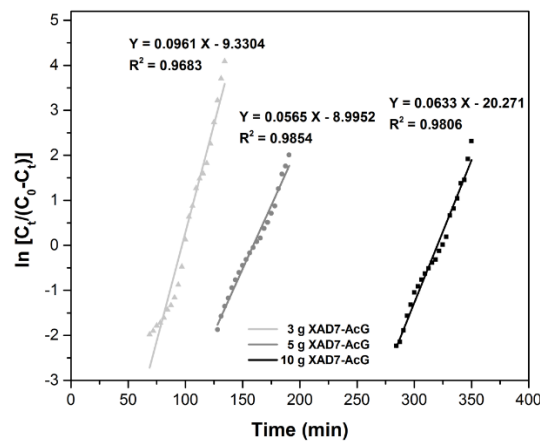


**Figure 6.** Yoon–Nelson plots for the adsorption of Au(III) in the fixed-bed column, at various amounts of adsorbent material.

The Thomas model [38] is the most commonly used model to describe the adsorption column performance and to establish breakthrough curves. It is frequently used to determine the adsorption capacity of the material. The Thomas equation is linearly expressed as:

$$\ln\left(\frac{C_0}{C_t} - 1\right) = \frac{k_{Th}q_{Th}m}{Q} - k_{Th}C_0t$$

where:  $C_0$ —is the solution concentration in the influent, ( $\text{mg L}^{-1}$ );  $C_t$ —is the solution concentration at time  $t$  in the effluent, ( $\text{mg L}^{-1}$ );  $k_{Th}$ —is the Thomas rate constant, ( $\text{L min}^{-1} \text{mg}^{-1}$ );  $q_{Th}$ —is the equilibrium compounds uptake per g of the resin, ( $\text{mg g}^{-1}$ );  $m$ —is the mass of adsorbent resin, ( $\text{g}$ );  $Q$ —is the flow rate, ( $\text{mL min}^{-1}$ ).

From the plot of  $\ln [C_0/(C_t - 1)] = f(t)$  are determined  $k_{Th}$  and  $q_{Th}$  (Figure 7). From the results obtained, it can be seen that the constant  $k_{Th}$  decreases as the adsorbent layer height in the column increases, due to the adsorption driving force given by the difference between the concentration of Au (III) adsorbed on the material and the Au (III) concentration in the solution [39–41].

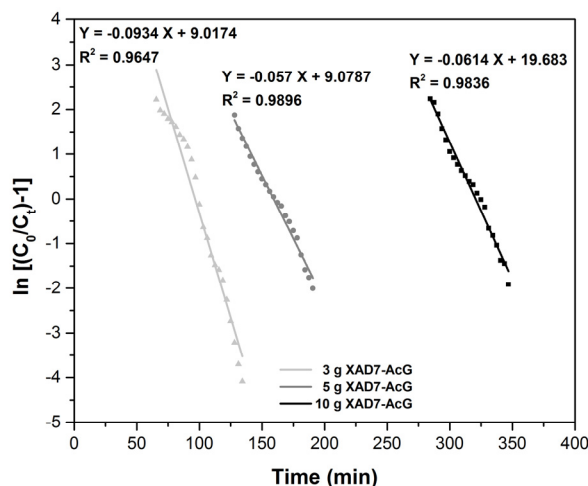


**Figure 7.** Thomas plots for the adsorption of Au (III) in the fixed-bed column, at various amounts of adsorbent material.

At the same time, it is observed that the regression coefficient  $R^2$  decreases, but the values are close to 1 and the adsorption capacity has about the same value, about  $13 \text{ (mg g}^{-1}\text{)}$ .

Another model reported in the literature for the adsorption study in the column is the Clark model. The main assumption of this model is the use of a mass-transfer concept in combination with the Freundlich isotherm [1,42,43].

The linearized expression of the Clark model is:

$$\ln\left(\left(\frac{C_0}{C_t}\right)^{n-1} - 1\right) = \ln A - rt$$

where:  $C_0$ —is the solution concentration in the influent, ( $\text{mg L}^{-1}$ );  $C_t$ —is the solution concentration at time  $t$  in the effluent, ( $\text{mg L}^{-1}$ );  $n$ —is the Freundlich constant determined experimentally in batch;  $r$ —is the Clark model constant, ( $\text{min}^{-1}$ );  $A$ —is the Clark model constant.

A previous batch adsorption study showed that the Freundlich constant was  $n = 2.5$  [26]. This value was used in the Clark model to estimate the model parameters for the Au (III) adsorption. The value of  $r$  and  $A$  parameters were evaluated by the slope and intercept of the linearized equation of the Clark model (Figure 8). The obtained correlation coefficients have good values ( $R^2 > 0.97$ ) for all the amounts of material studied. The increase of amounts of material leads to decrease of parameter  $r$  value and to increase of value of  $A$  parameter.

The difference in the models was based on the set parameters, not on matching the experimental data. Column parameters of all tested models for the adsorption process in dynamic regime are presented in Table 1. It can be observed that all the applied four models fitted to a satisfactory extent the variation in the amount of adsorbent, respectively, the variation of the material layer height. All models have shown good values of the correlation coefficient which suggests their validity in this investigation. Additionally, in the case of the Thomas model, the adsorption capacity has about the same value for all the amounts of adsorbent used, about  $13 \text{ (mg g}^{-1}\text{)}$ . Therefore, it can be assumed that this model best describes the mechanism of the adsorption process in a dynamic regime [41].



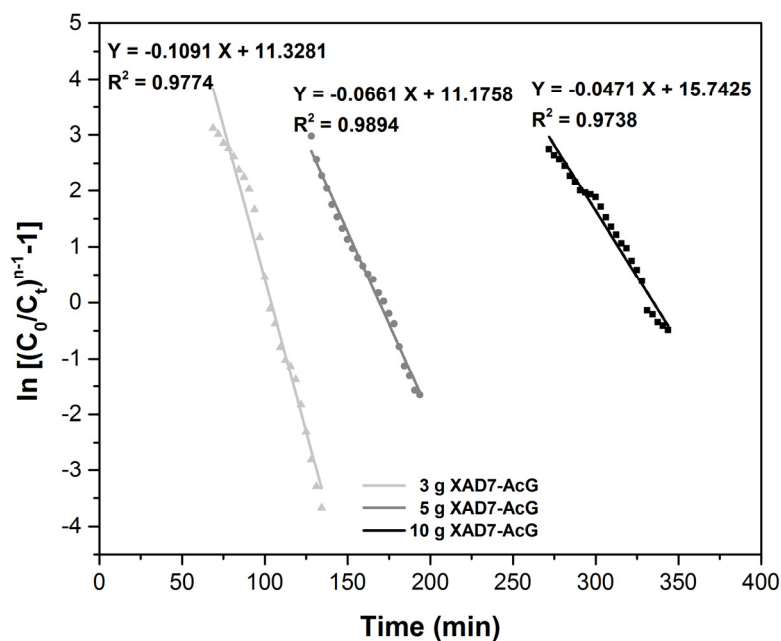


**Figure 8.** Clark plots for the adsorption of Au (III) in the fixed-bed column, at various amounts of adsorbent material.

**Table 1.** Au (III) adsorption process parameters on fixed bed column.

Column Parameters				
<b>Bohart-Adams Model</b>	Material Amount (g)	$K_{B-A}$ (L mg <sup>-1</sup> min <sup>-1</sup> )	$N_0$ (mg L <sup>-1</sup> )	$R^2$
	10	$8.6 \times 10^{-4}$	1099.6	0.9644
	5	$7.5 \times 10^{-4}$	1141.9	0.9747
	3	$7.4 \times 10^{-4}$	1146.2	0.9503
<b>Yoon-Nelson Model</b>	Material Amount (g)	$K_{Y-N}$ (min <sup>-1</sup> )	T (min)	$R^2$
	10	0.0633	320.23	0.9806
	5	0.0565	159.2	0.9854
	3	0.0253	97.09	0.9683
<b>Thomas Model</b>	Material Amount (g)	$K_{Th}$ (L mg <sup>-1</sup> min <sup>-1</sup> )	$q_{Th}$ (mg g <sup>-1</sup> )	$R^2$
	10	$1.02 \times 10^{-3}$	13.376	0.9836
	5	$1.05 \times 10^{-3}$	13.379	0.9896
	3	$1.56 \times 10^{-3}$	13.520	0.9647
<b>Clark Model</b>	Material Amount (g)	r (min <sup>-1</sup> )	A	$R^2$
	10	0.0471	$68.5 \times 10^{-5}$	0.9738
	5	0.0661	$70.9 \times 10^{-3}$	0.9894
	3	0.1091	$82.4 \times 10^{-3}$	0.9774

Maximum adsorption capacities of previously studied adsorbents for Au (III) recovery are presented in Table 2. The value of this parameter is comparable to those previously reported in the literature, even higher than other similar adsorbents.

The mechanism of Au (III) recovery by adsorption is that in most cases ionic species come into contact with the solid surface of the material with adsorbent properties. Adsorption is determined by Van der Waals forces, which are manifested between the material with adsorbent properties and the Au (III) ion. The predominant species at pH = 2 is  $AuCl_4^-$ . This species does not adsorb to the XAD7-AcG surface in a certain position, but moves freely, by translation, at the interface. In the aqueous solution there are three types of interaction considered competitive, namely: (i) the

interaction between Au (III) ions and water; (ii) the interaction between Au (III) ions and the surface of the material with adsorbent properties and (iii) the interaction between water and the surface of the XAD7-AcG material. The efficiency of the physical adsorption process is determined by the strength of the metal ion–adsorbent surface interactions compared to the strength of the surface adsorbent–water interactions.

**Table 2.** Maximum adsorption capacities of previously studied adsorbents.

Adsorbent	Adsorption Capacity ( $\text{mg g}^{-1}$ )	Reference
Sericin and algininate particle-based adsorbent SAPAS	57.91	[44]
Amberlite XAD7 type functionalized with L-glutamic acid (XAD7-AcG).	13.5	This study
Carboxymethyl chitin	11.86	[45]
Macadamia-activated carbon (MAC)	9.13	[46]
Magnetic nickeliferous pyrrhotite	6.9	[47]
Cotton cellulose	1.22 *	[48]
Activated carbon F400	0.25 **	[22]

\* Original report is 6.21 (mmol/g). \*\* Original report is 250 ( $\mu\text{g/g}$ ).

### 3.3. Desorption Studies

Very important for an adsorbent material is the number of adsorption–desorption cycles to which it can be subjected. The profitability, feasibility and sustainability of an adsorption process is essentially influenced by the regeneration possibilities of the adsorbent material. The desorption studies prove the practical applicability of the adsorption process, regarding the reuse of the fixed layer of adsorbent material in the column, after exhaustion [37,49].

In this study,  $\text{HNO}_3$  5% as desorption agent was used in five adsorption–desorption cycles. The results presented in Figures 9 and 10 indicate that, with the increase of the adsorption–desorption cycles numbers there are subsequent losses in the adsorbent mass, so that the degree of desorption varies between 84% and 34% from cycle 1 to cycle 5.

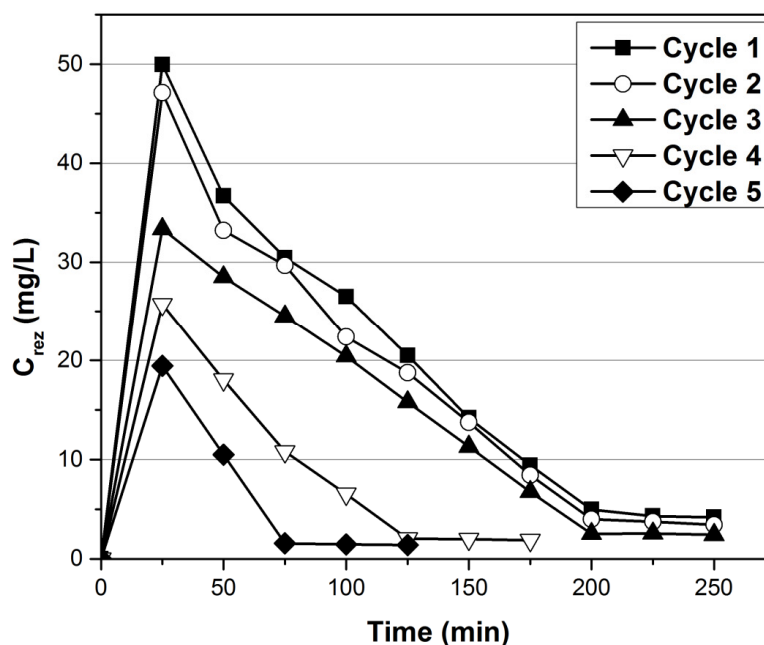


**Figure 9.** Desorption curves of Au (III) adsorbed on XAD7-AcG (10 g amounts), in five adsorption–desorption cycles.

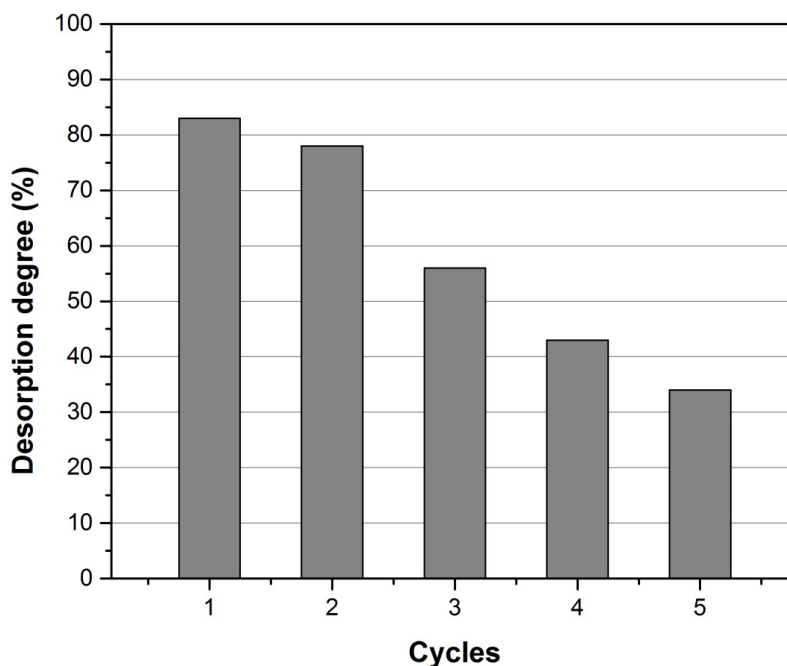


**Figure 10.** Comparative desorption degree of HNO<sub>3</sub> 5%, as desorption agent, to elute Au (III) ions from XAD7-AcG adsorbent material, in consecutive cycles.

Au(III) remaining on the adsorbent material, after the 5 cycles of adsorption–desorption, can be recovered in metallic form by calcination, at 873 K for 240 min, at a heating rate of 5 K/min, using controlled air oven furnaces, removing the organic part and with only the metal remaining, according to some previous studies [26].

A simple cost estimate (taking into account the price of gold on the market) led to the conclusion that for 100 g of adsorbent material, used in 5 cycles of adsorption–desorption and then calcined, the profit would be about 125 euros.

#### 4. Conclusions

In this paper, the recovery of Au (III) ions from used solutions resulting from galvanic coating processes, by adsorption, in dynamic regime, using a fixed-bed column, was studied. The adsorbent was a new material obtained by impregnation of a commercial resin, Amberlite XAD7, with L-glutamic acid, which has in its structure functional groups of –NH<sub>2</sub> and –COOH. In order to establish the mechanism of the dynamic adsorption process, the experimental data were modeled using the Bohart–Adams, Yoon–Nelson, Thomas and Clark models.

The Thomas model best describes the recovery process of Au (III) by adsorption in dynamic regime. The effluent flow rate, the column height, the material mass in the column and the time required to break through the column were taken into account.

The XAD7-AcG adsorbent material can be used in five adsorption–desorption cycles, until the process is no longer efficient. The Au (III) retained in the adsorbent material can be recovered by calcination, removing the organic part and leaving only the metal [14]. The adsorption capacity of the XAD7-AcG adsorbent material is large enough for the Au (III) recovery process to be cost effective.

**Author Contributions:** Conceptualization, A.N., M.M., M.C., V.M.; Methodology, A.N., M.M.; Software, V.M., G.M.; Validation, A.N., P.N., N.D.; Formal Analysis, A.N., N.D., G.M.; Investigation, A.N., M.M., M.C., V.M.; Resources, A.N., P.N.; Writing—Original Draft Preparation, A.N., M.C.; Writing—Review and Editing, A.N., G.M.; Visualization, A.N., N.D., P.N.; Supervision, A.N.; Project Administration, A.N., M.C.; Funding Acquisition, A.N. All authors have read and agreed to the published version of the manuscript.

**Funding:** This work was supported by a grant of the Romanian Minister of Research and Innovation, project number 10PFE/16.10.2018, PERFORM-TECH-UPT—The increasing of the institutional performance of the Polytechnic

University of Timisoara by strengthening the research, development and technological transfer capacity in the field of “Energy, Environment and Climate Change”, within Program 1—Development of the national system of Research and Development, Subprogram 1.2—Institutional Performance—Institutional Development Projects—Excellence Funding Projects in RDI, PNCDI III”.

**Conflicts of Interest:** The authors declare no conflict of interest.

## References

1. Patel, H. Fixed-bed column adsorption study: A comprehensive review. *Appl. Water. Sci.* **2019**, *9*, 45. [[CrossRef](#)]
2. Dabrowski, A. Adsorption—From theory to practice. *Adv. Colloid Interface Sci.* **2001**, *93*, 135–224. [[CrossRef](#)]
3. Selim, K.A.; Youssef, M.A.; Abd El-Rahiem, F.H.; Hassan, M.S. Dye removal using some surface modified silicate minerals. *Int. J. Min. Sci. Technol.* **2014**, *24*, 183–189. [[CrossRef](#)]
4. Kafshgari, F.; Keshkar, A.R.; Mousavian, M.A. Study of Mo (VI) removal from aqueous solution: Application of different mathematical models to continuous biosorption data. *Iran. J. Environ. Health Sci. Eng.* **2013**, *10*, 14. [[CrossRef](#)] [[PubMed](#)]
5. Miralles, N.; Valderrama, C.; Casas, I.; Martinez, M.; Florido, A. Cadmium and Lead Removal from Aqueous Solution by Grape Stalk Wastes: Modeling of a Fixed-Bed Column. *J. Chem. Eng. Data* **2010**, *55*, 3548–3554. [[CrossRef](#)]
6. Ramesh, A.; Hasegawa, H.; Sugimoto, W.; Maki, T.; Ueda, K. Adsorption of gold(III), platinum(IV) and palladium(II) onto glycine modified crosslinked chitosan resin. *Bioresour. Technol.* **2008**, *99*, 3801–3809. [[CrossRef](#)]
7. Spitzer, M.; Rodnei, B. Selective electrochemical recovery of gold and silver from cyanide aqueous effluents using titanium and vitreous carbon cathodes. *Hydrometallurgy* **2004**, *74*, 233–242. [[CrossRef](#)]
8. Syed, S. Recovery of gold from secondary sources—A review. *Hydrometallurgy* **2012**, *115–116*, 30–51. [[CrossRef](#)]
9. Cui, J.; Zhang, L. Metallurgical recovery of metals from electronic waste: A review. *J. Hazard. Mater.* **2008**, *158*, 228–256. [[CrossRef](#)]
10. Fleming, C.A. Hydrometallurgy of precious metals recovery. *Hydrometallurgy* **1992**, *30*, 127–162. [[CrossRef](#)]
11. Rhee, K.I.; Lee, J.C.; Lee, C.K.; Joo, K.H.; Yoon, J.K.; Kang, H.R.; Kim, Y.S.; Sohn, H.J. A Recovery of Gold from Electronic Scrap by Mechanical Separation, Acid Leaching and Electrowinning. In *Recycling Metals and Engineered Materials*; Queneau, P.B., Peterson, R.D., Eds.; TMS Publication: Pittsburgh, PA, USA, 1995; pp. 469–478.
12. Yap, C.Y.; Mohamed, N. An electro-generative process for the recovery of gold from cyanide solutions. *Chemosphere* **2007**, *67*, 1502–1510. [[CrossRef](#)] [[PubMed](#)]
13. Hoffmann, J.E. Recovering precious metals from electronic scrap. *J. Miner. Metall. Mater. Soc.* **1992**, *44*, 43–48. [[CrossRef](#)]
14. Lee, J.C.; Song, H.T.; Yoo, J.M. Present status of the recycling of waste electrical and electronic equipment in Korea. *Resour. Conserv. Recycl.* **2007**, *50*, 380–397. [[CrossRef](#)]
15. Mack, C.; Wilhelmi, B.; Duncan, J.R.; Burgess, J.E. Biosorption of precious metals. *Biotechnol. Adv.* **2007**, *25*, 264–271. [[CrossRef](#)] [[PubMed](#)]
16. Safarzadeh, M.S.; Bafghi, M.S.; Moradkhani, D.; Ilkhchi, M.O. A review on hydrometallurgical extraction and recovery of cadmium from various resources. *Miner. Eng.* **2007**, *20*, 211–220. [[CrossRef](#)]
17. Sum, E.Y.L. The Recovery of Metals from Electronic Scrap. *J. Miner. Metall. Mater. Soc.* **1991**, *43*, 53–61. [[CrossRef](#)]
18. Jafari, S.; Wilson, B.P.; Hakalahti, M.; Tammel, T.; Kontturi, E.; Lundstrom, M.; Sillanpaa, M. Recovery of Gold from Chloride Solution by TEMPO-Oxidized Cellulose Nanofiber Adsorbent. *Sustainability* **2019**, *11*, 1406. [[CrossRef](#)]
19. Li, Y.; Zhou, Y.; Zhou, Y.; Lei, J.; Pu, S. Cyclodextrin modified filter paper for removal of cationic dyes/Cu ions from aqueous solutions. *Water Sci. Technol.* **2018**, *78*, 2553–2563. [[CrossRef](#)]
20. Liu, Q.; Zhou, Y.; Lu, J.; Zhou, Y. Novel cyclodextrin-based adsorbents for removing pollutants from wastewater: A critical review. *Chemosphere* **2020**, *241*, 125043. [[CrossRef](#)]

21. Syed, S. A green technology for recovery of gold from non-metallic secondary sources. *Hydrometallurgy* **2006**, *82*, 48–53. [[CrossRef](#)]
22. Vences-Alvarez, E.; Razo-Flores, E.; Lazaro, I.; Briones-Gallardo, R.; Velasco-Martinez, G.; Rangel-Mendez, R. Gold recovery from very dilute solutions from a mine in closing process: Adsorption-desorption onto carbon materials. *J. Mol. Liq.* **2017**, *240*, 549–555. [[CrossRef](#)]
23. Bui, T.H.; Lee, W.; Jeon, S.B.; Kim, K.W.; Lee, Y. Enhanced Gold(III) adsorption using glutaraldehyde-crosslinked chitosan beads: Effect of crosslinking degree on adsorption selectivity, capacity, and mechanism. *Sep. Purif. Technol.* **2020**, *248*, 116989. [[CrossRef](#)]
24. Yi, Q.; Fan, R.; Xie, F.; Min, H.; Zhang, Q.; Luo, Z. Selective Recovery of Au(III) and Pd(II) from Waste PCBs Using Ethylenediamine Modified Persimmon Tannin Adsorbent. *Procedia Environ. Sci.* **2016**, *31*, 185–194. [[CrossRef](#)]
25. Cortina, J.L.; Warshawsky, A. Developments in Solid-Liquid Extraction by Solvent-Impregnated Resins. In *Ion Exchange and Solvent Extraction*; Marinsky, J.A., Marcus, Y., Eds.; Marcel Dekker Inc.: New York, NY, USA, 1997; pp. 195–293.
26. Mihailescu, M.; Negrea, A.; Ciopec, M.; Davidescu, C.M.; Negrea, P.; Duteanu, N.; Rusu, G. Gold (III) adsorption from dilute waste solutions onto Amberlite XAD7 resin modified with L-glutamic acid. *Sci. Rep.* **2019**, *9*, 8757. [[CrossRef](#)] [[PubMed](#)]
27. Vasanth Kumar, K.; Subanandam, K.; Bhagavanulu, D.V.S. Making GAC sorption economy. *Pollut. Res.* **2004**, *23*, 439–444.
28. Gupta, V.K.; Ali, I. *Environmental Water: Advances in Treatment, Remediation and Recycling*; Elsevier: Amsterdam, The Netherlands, 2013.
29. Crittenden, B.; Thomas, W.J. *Adsorption Technology and Design*; Butterworth-Heinemann: Oxford, UK, 1998.
30. Chowdhury, Z.Z.; Zain, S.M.; Rashid, A.K.; Rafique, R.F.; Khalid, K. Breakthrough Curve Analysis for Column Dynamics Sorption of Mn(II) Ions from Wastewater by Using *Mangostana garcinia* Peel-Based Granular-Activated Carbon. *J. Chem.* **2013**, *2013*, 959761. [[CrossRef](#)]
31. Hasanzadeh, M.; Ansari, R.; Ostovar, F. Synthesis and application of CeO<sub>2</sub>/sawdust nanocomposite for removal of As(III) ions from aqueous solutions using a fixed bed column system. *Glob. NEST J.* **2016**, *19*, 7–16.
32. Shafeeyan, M.S.; Daud, W.M.A.W.; Shamiri, A. A review of mathematical modeling of fixed-bed columns for carbon dioxide adsorption. *Chem. Eng. Res. Des.* **2014**, *92*, 961–988. [[CrossRef](#)]
33. Yang, Q.; Zhong, Y.; Li, X.; Li, X.; Luo, K.; Wua, X.; Chen, H.; Liu, Y.; Zeng, G. Adsorption-coupled reduction of bromate by Fe(II)–Al(III) layered double hydroxide in fixed-bed column: Experimental and breakthrough curves analysis. *J. Ind. Eng. Chem.* **2015**, *28*, 54–59. [[CrossRef](#)]
34. Han, R.; Wang, Y.; Zhao, X.; Wang, Y.; Xie, F.; Cheng, J. Adsorption of methylene blue by phoenix tree leaf powder in a fixed-bed column: Experiments and prediction of breakthrough curves. *Desalination* **2009**, *245*, 284–297. [[CrossRef](#)]
35. Bohart, G.S.; Adams, E.Q. Some aspects of the behavior of charcoal with respect to chlorine. *J. Am. Chem. Soc.* **1920**, *42*, 523–544. [[CrossRef](#)]
36. Woumfo, E.D.; Siewe, J.M.; Njopwouo, D. A fixed-bed column for phosphate removal from aqueous solutions using an andosol-bagasse mixture. *J. Environ. Manag.* **2015**, *151*, 450–460. [[CrossRef](#)] [[PubMed](#)]
37. Vilvanathan, S.; Shanthakumar, S. Column adsorption studies on nickel and cobalt removal from aqueous solution using native and biochar form of *Tectona grandis*. *Environ. Prog. Sustain.* **2017**, *36*, 1030–1038. [[CrossRef](#)]
38. Thomas, H.C. Heterogeneous Ion Exchange in a Flowing System. *J. Am. Chem. Soc.* **1944**, *66*, 1664–1667. [[CrossRef](#)]
39. Han, R.; Zhang, J.; Zou, W.; Xiao, H.; Shi, J.; Liu, H. Biosorption of copper(II) and lead(II) from aqueous solution by chaff in a fixed-bed column. *J. Hazard. Mater.* **2006**, *133*, 262–268. [[CrossRef](#)] [[PubMed](#)]
40. Han, R.; Wang, Y.; Zou, W.; Wang, Y.; Shi, J. Comparison of linear and nonlinear analysis in estimating the Thomas model parameters for methylene blue adsorption onto natural zeolite in fixed-bed column. *J. Hazard. Mater.* **2007**, *145*, 331–335. [[CrossRef](#)] [[PubMed](#)]
41. Mondal, S.; Aikat, K.; Halder, G. Ranitidine hydrochloride sorption onto superheated steam activated biochar derived from mung bean husk in fixed bed column. *J. Environ. Chem. Eng.* **2016**, *4*, 488–497. [[CrossRef](#)]

42. Dlugosz, O.; Banach, M. Sorption of  $\text{Ag}^+$  and  $\text{Cu}^{2+}$  by Vermiculite in a Fixed-Bed Column: Design, Process Optimization and Dynamics Investigations. *Appl. Sci.* **2018**, *8*, 2221. [[CrossRef](#)]
43. Madan, S.S.; De, B.S.; Wasewar, K.L. Adsorption performance of packed bed column for benzylformic acid removal using  $\text{CaO}_2$  nanoparticles. *Chem. Data Collect.* **2019**, *23*, 100267. [[CrossRef](#)]
44. Santos, N.T.; Landers, R.; da Silva, M.G.C.; Vieira, M.G.A. Adsorption of Gold Ions onto Sericin and Alginate Particles Chemically Crosslinked by Proanthocyanidins: A Complete Fixed-Bed Column Study. *Ind. Eng. Chem. Res.* **2020**, *59*, 318–328. [[CrossRef](#)]
45. Wasikiewicz, J.M.; Nagasawa, N.; Tamada, M.; Mitomo, H.; Yoshii, F. Adsorption of metal ions by carboxymethylchitin and carboxymethylchitosan hydrogels. *Nucl. Instrum. Methods Phys. Res. B* **2005**, *236*, 617–623. [[CrossRef](#)]
46. Tsolele, R.; Mtunzi, F.M.; Klink, M.J.; Pakade, V.E. An alternative low-cost adsorbent for gold recovery from cyanide-leached liquors: Adsorption isotherm and kinetic studies. *Adsorp. Sci. Technol.* **2018**, *37*, 3–23. [[CrossRef](#)]
47. Calderon, A.R.M.; Alorro, R.D.; Tadesse, B.; Yoo, K.; Tabelin, C.B. Repurposing of nickeliferous pyrrhotite from mine tailings as magnetic adsorbent for the recovery of gold from chloride solution. *Resour. Conserv. Recycl.* **2020**, *161*, 104971. [[CrossRef](#)]
48. Pangen, B.; Paudyal, H.; Inoue, K.; Kawakita, H.; Ohto, K.; Alam, S. Selective recovery of gold(III) using cotton cellulose treated with concentrated sulfuric acid. *Cellulose* **2012**, *19*, 381–391. [[CrossRef](#)]
49. Abdolali, A.; Ngo, H.H.; Guo, W.; Zhou, J.L.; Zhang, J.; Liang, S.; Chang, S.W.; Nguyen, D.D.; Liu, Y. Application of a breakthrough biosorbent for removing heavy metals from synthetic and real wastewaters in a lab-scale continuous fixed-bed column. *Bioresour. Technol.* **2017**, *229*, 78–87. [[CrossRef](#)] [[PubMed](#)]



© 2020 by the authors. Licensee MDPI, Basel, Switzerland. This article is an open access article distributed under the terms and conditions of the Creative Commons Attribution (CC BY) license (<http://creativecommons.org/licenses/by/4.0/>).